Supporting Information

Accelerating filtration by introducing oscillation paradigm and its atomistic origin

Na Li,[a] Zemeng Feng,[a] Huijuan Lin,[a] Jixin Zhu,[b] Kui Xu [a*]*

[a] School of Flexible Electronics (Future Technologies) & Institute of Advanced Materials (IAM), Nanjing Tech University (NanjingTech), 30 South Puzhu Road, Nanjing 211816, P. R. China

[b] State Key Laboratory of Fire Science, University of Science and Technology of China, 443 Huangshan Road, Hefei, 230027 P. R. China

Corresponding Authors

*Kui Xu, E-mail: iamkxu@njtech.edu.cn

*Jixin Zhu, E-mail: zhujixin@ustc.edu.cn

Section S1. Synthesis methods and structural properties of COF-O materials.

The precursor is cyclohexanehexone and aromatic tetramines with benzoquinone. The monomeric unit is shown in Fig. 1c. It was built based on Materials Studio and then optimized by the Cambridge Sequential Total Energy Package (CASTEP) with the exchange correlation functional of the general gradient approximation (GGA) formulated by Perdew-Burke-Ernzerhof (PBE). the diameter of COF-O is 1.2 nm, and the corresponding effective diameter is about 0.91 nm.

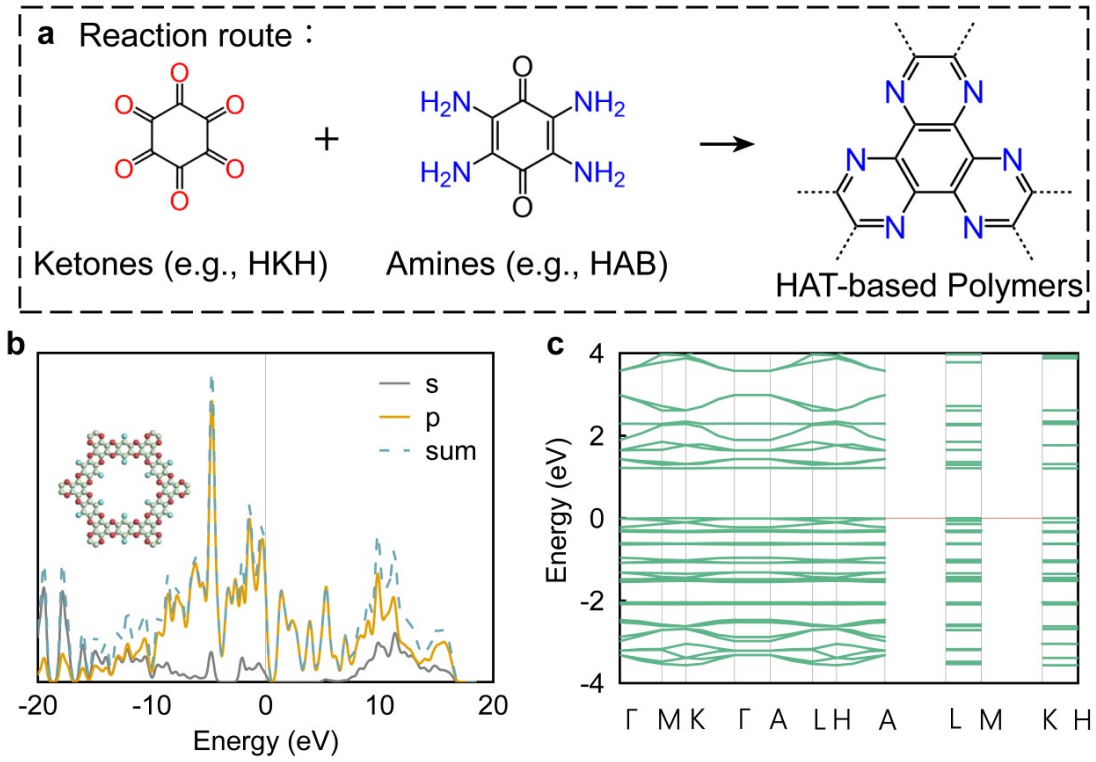

Fig. S1 Synthetic route towards COF-O. (a) Projected electron density (PDOS) (b) and the total electron density (TDOS) (c).

Section S2. The calculations details of classical molecular dynamics.

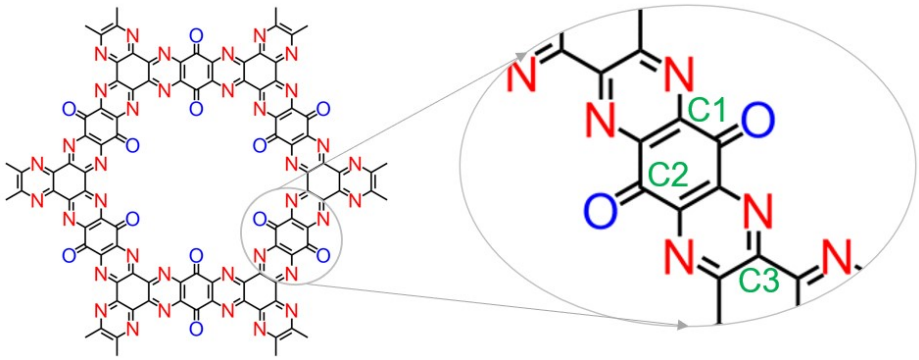

Element	Charge(e)	ε/kcal.mol^{-1}	δ/nm
C1	0.096	0.385	0.10500
C2	0.232	0.385	0.10500
C3	0.139	0.385	0.10500
O (COF)	-0.236	0.350	0.06000
N	-0.233	0.366	0.06900
Na	1.00	0.130	0.23500
Cl	-1.00	0.1000	0.44000
O (H_2O)	-0.848	0.1544	0.31655
H (H_2O)	0.424	0.0000	0.00000

Fig. S2 The Lennard-Jones parameters used in simulations, Lorentz−Berthelot mixing rules were employed for the nonbonded interactions.

Section S3. The permeability and selectivity for COF-O with 10% horizontal offset.

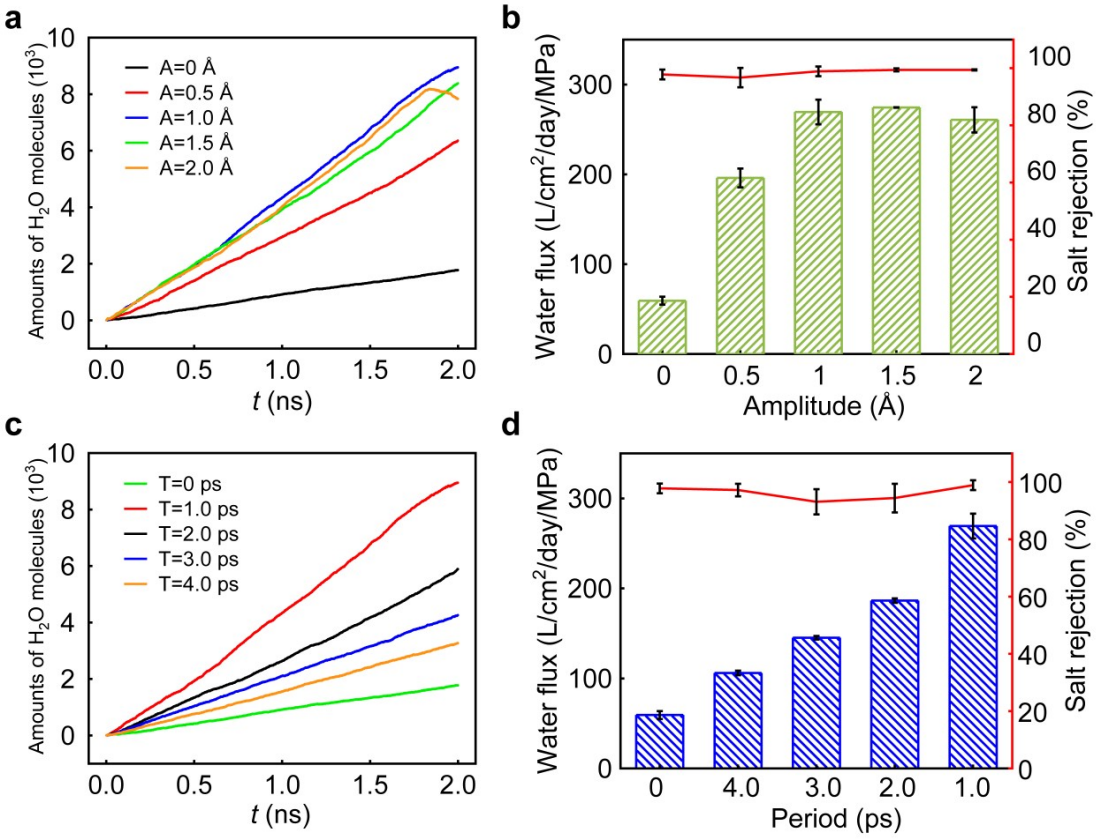

Fig. S3 The amounts of penetrated water molecules as a function of time at different amplitudes (0 - 2.0 Å) (a) and periods (0 - 4.0 ps) (c). Water flux and salt rejection as functions of amplitudes (0 - 2.0 Å) (b) and periods (0 - 4.0 ps) (d).

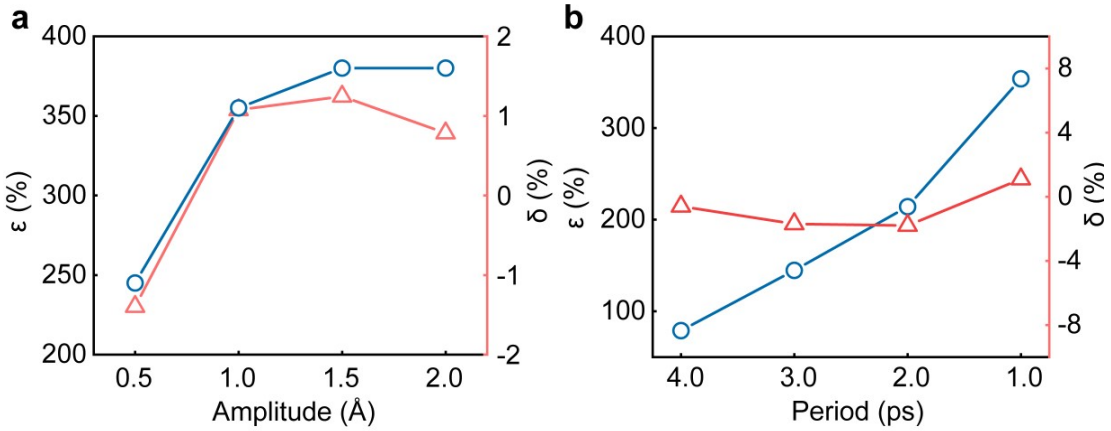

Fig. S4 Enhancement rate of water flux and salt rejection as functions of amplitudes (a) and periods (b).

Section S4. The permeability and selectivity for COF-O with 20% horizontal offset.

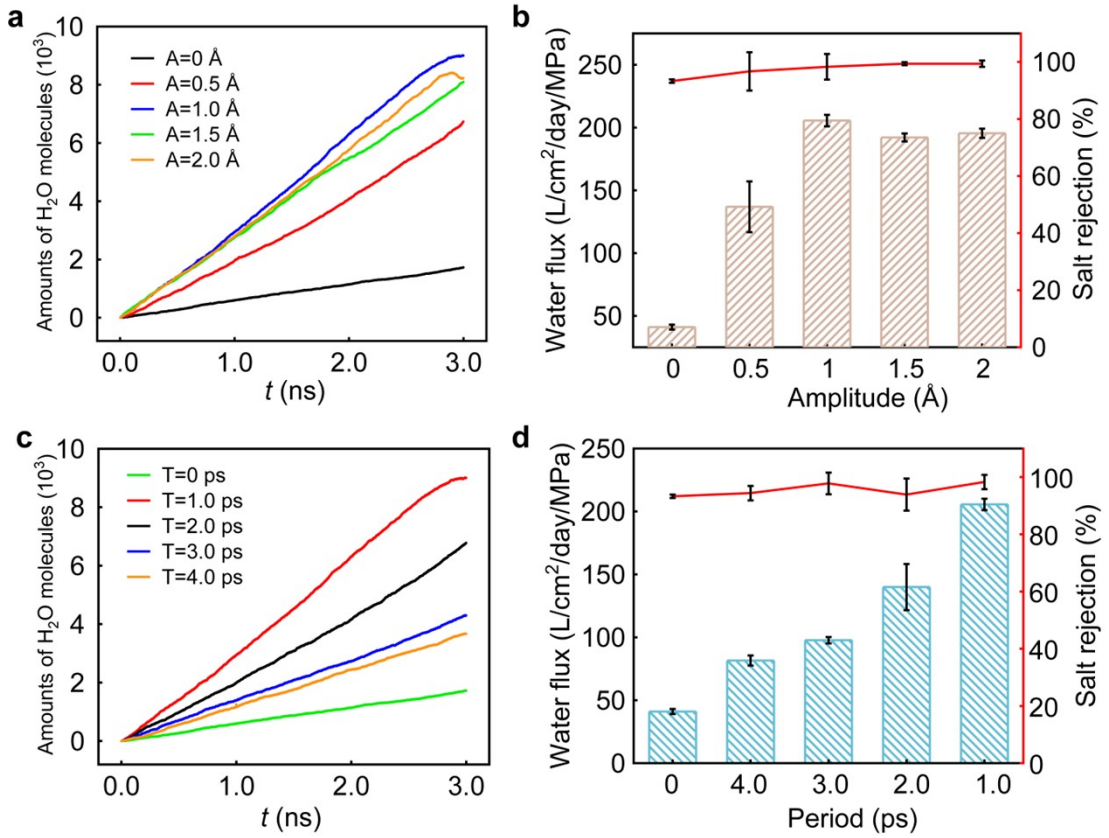

Fig. S5 The amounts of penetrated water molecules as a function of time at different amplitudes (0 - 2.0 Å) (a) and periods (0 - 4.0 ps) (c). Water flux and salt rejection as functions of amplitudes (0 - 2.0 Å) (b) and periods (0 - 4.0 ps) (d).

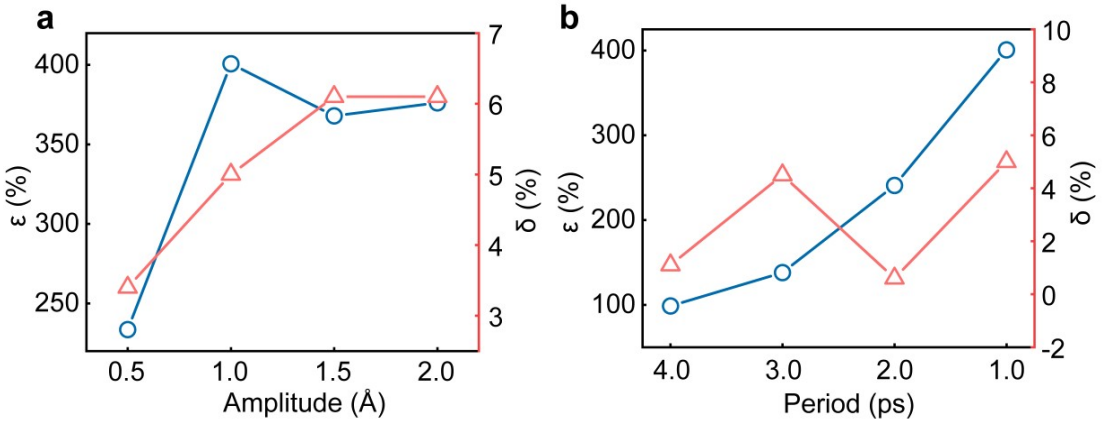

Fig. S6 Enhancement rate of water flux and salt rejection as functions of amplitudes (a) and periods (b).

Section S5. The permeability and selectivity for COF-O with 26% horizontal offset.

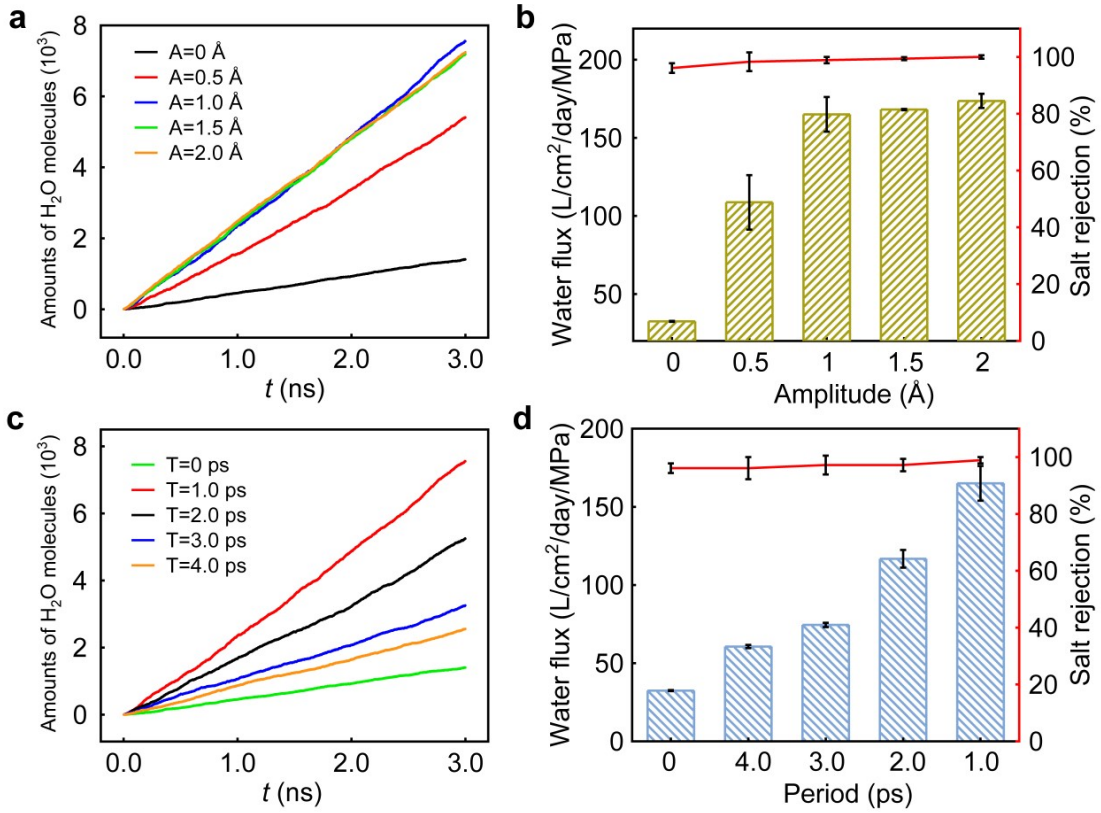

Fig. S7 The amounts of penetrated water molecules as a function of time at different amplitudes (0 - 2.0 Å) (a) and periods (0 - 4.0 ps) (c). Water flux and salt rejection as functions of amplitudes (0 - 2.0 Å) (b) and periods (0 - 4.0 ps) (d).

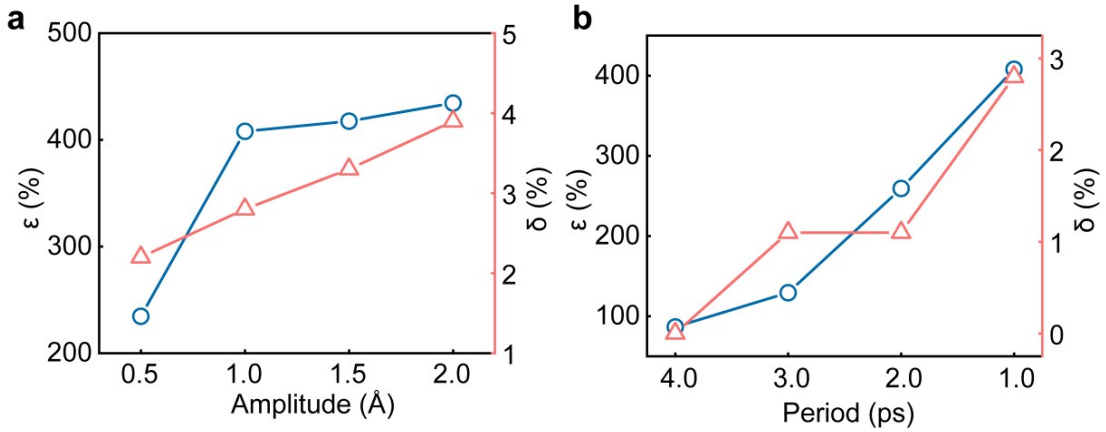

Fig. S8 Enhancement rate of water flux and salt rejection as functions of amplitudes (a) and periods (b).

Section S6. The permeability and selectivity for COF-O with 32% horizontal offset.

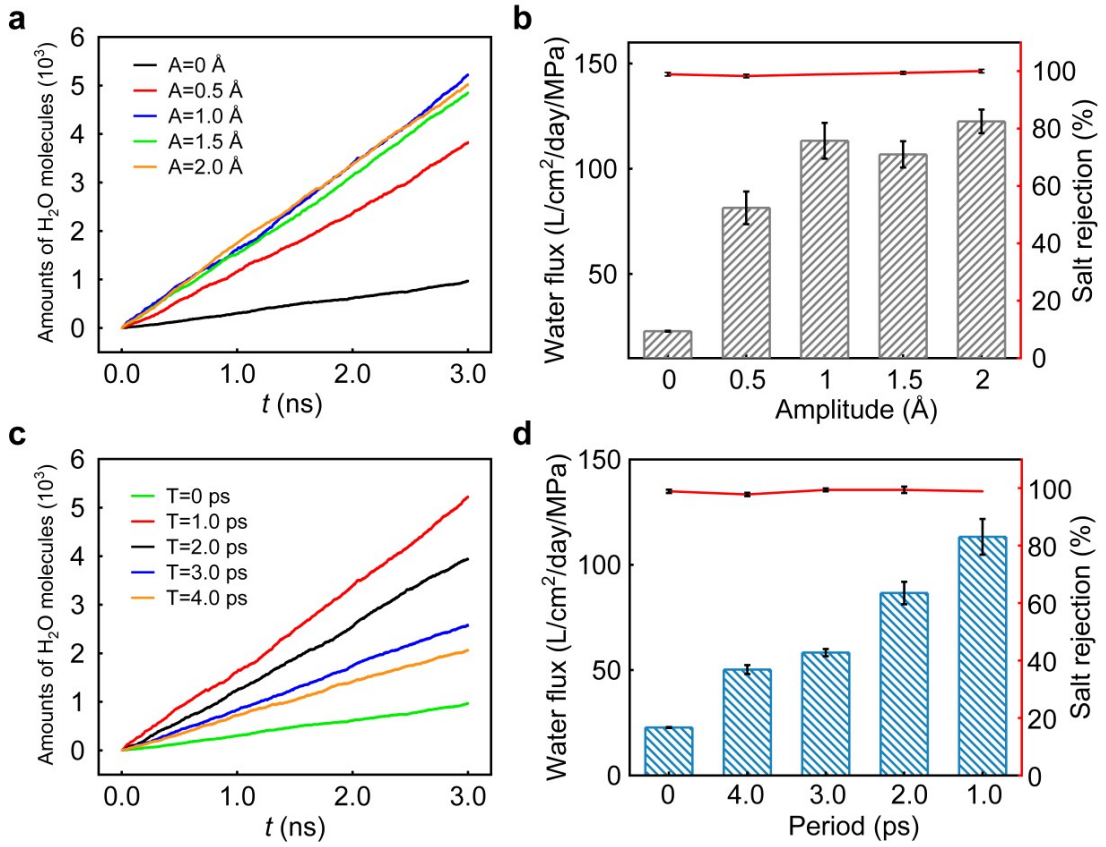

Fig. S9 The amounts of penetrated water molecules as a function of time at different amplitudes (0 - 2.0 Å) (a) and periods (0 - 4.0 ps) (c). Water flux and salt rejection as functions of amplitudes (0 - 2.0 Å) (b) and periods (0 - 4.0 ps) (d).

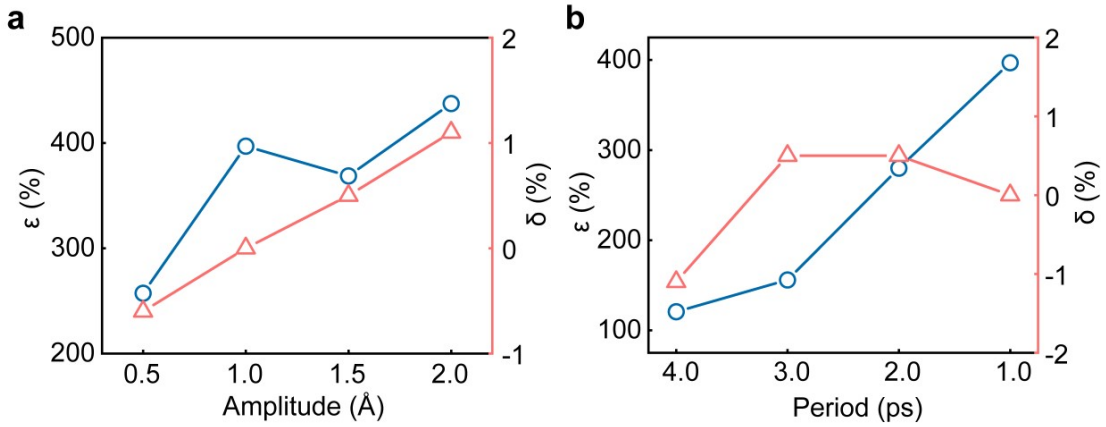

Fig. S10 Enhancement rate of water flux and salt rejection as functions of amplitudes (a) and periods (b).

Section S7. The permeability and selectivity for COF-O with 38% horizontal offset.

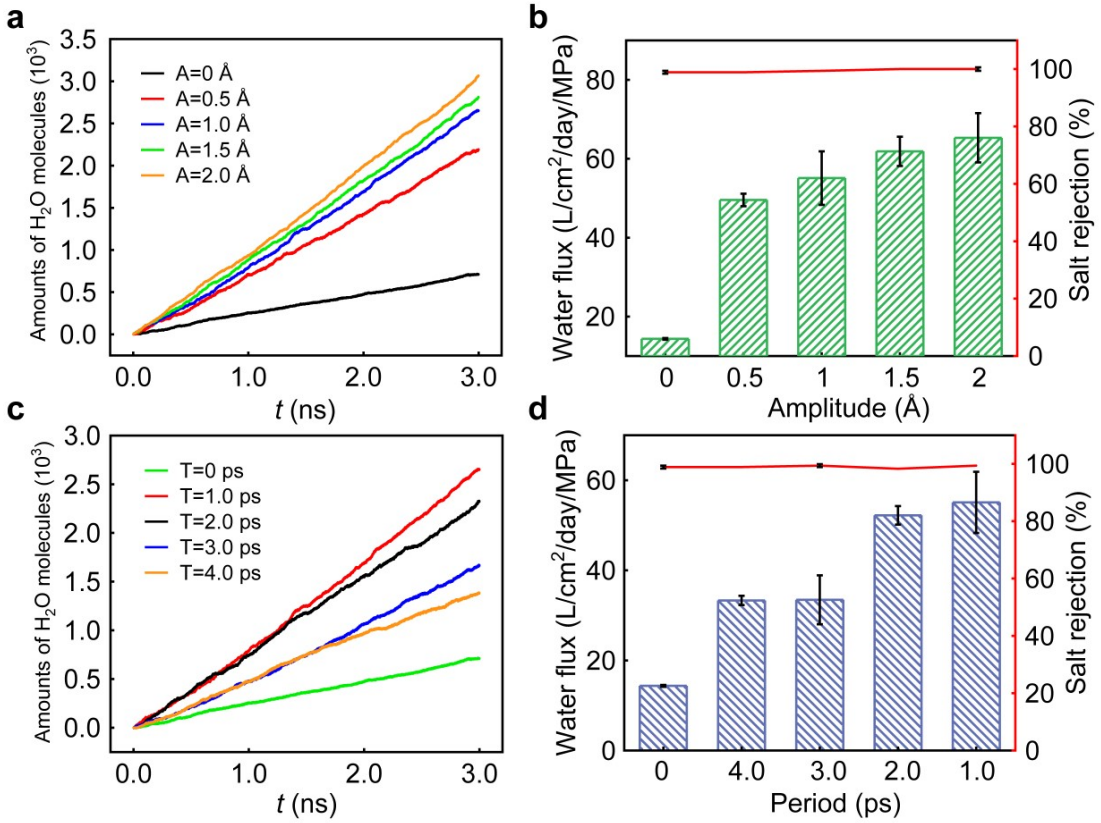

Fig. S11 The amounts of penetrated water molecules as a function of time at different amplitudes (0 - 2.0 Å) (a) and periods (0 - 4.0 ps) (c). Water flux and salt rejection as functions of amplitudes (0 - 2.0 Å) (b) and periods (0 - 4.0 ps) (d).

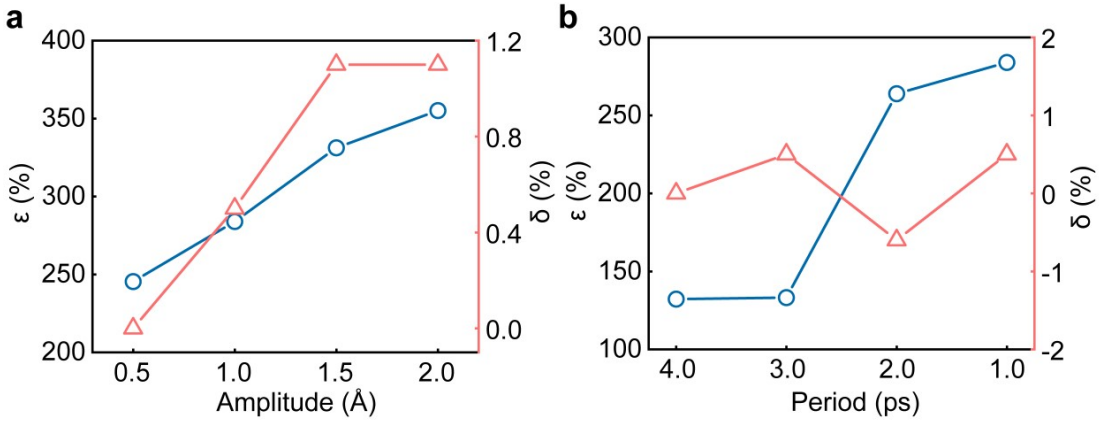

Fig. S12 Enhancement rate of water flux and salt rejection as functions of amplitudes (a) and periods (b).

Section S8. The permeability and selectivity for COF-O with 44% horizontal offset.

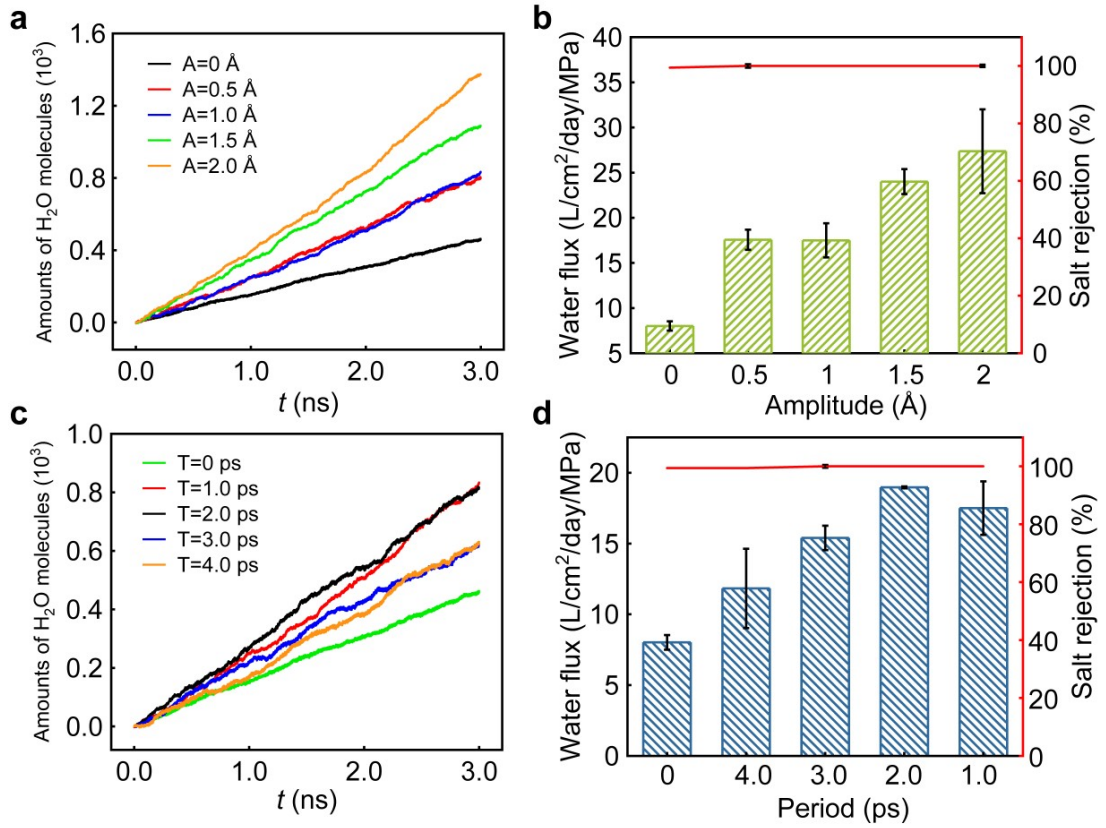

Fig. S13 The amounts of penetrated water molecules as a function of time at different amplitudes (0 - 2.0 Å) (a) and periods (0 - 4.0 ps) (c). Water flux and salt rejection as functions of amplitudes (0 - 2.0 Å) (b) and periods (0 - 4.0 ps) (d).

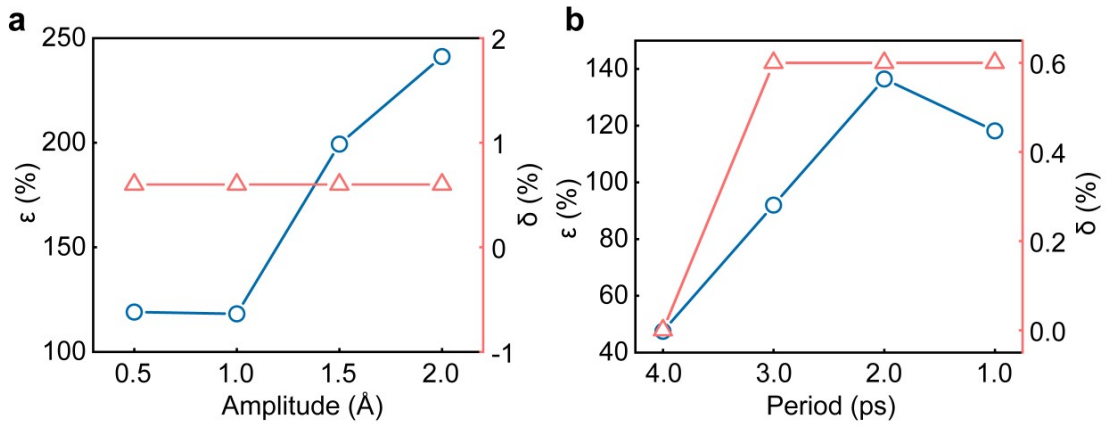

Fig. S14 Enhancement rate of water flux and salt rejection as functions of amplitudes (a) and periods (b).

Section S9. Model diagram of bilayer COF-O nanosheets with several different offsets of 0%-50%.

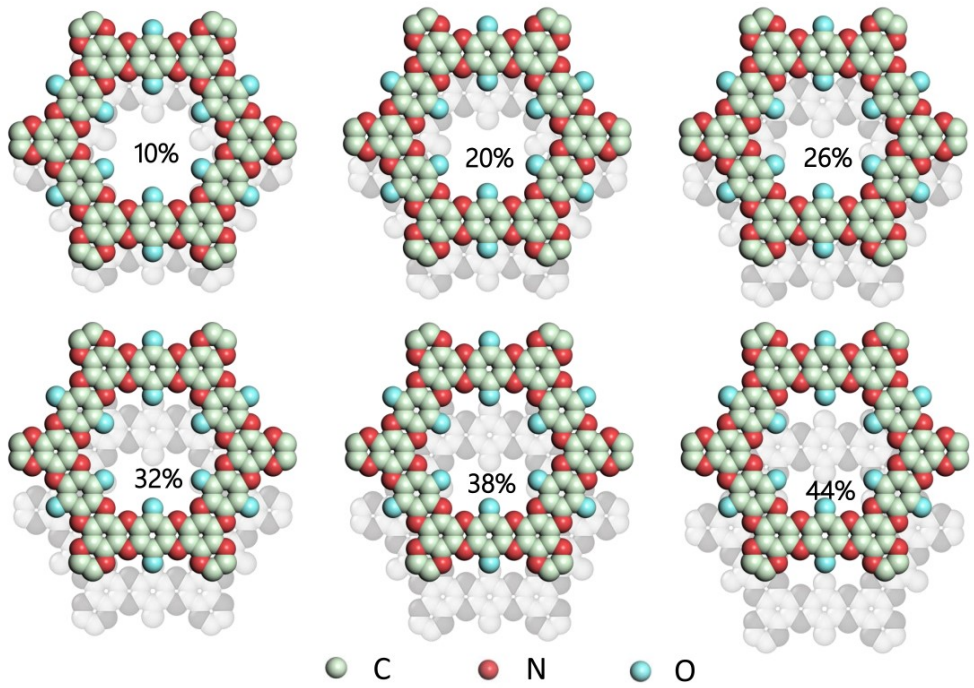

Fig. S15 Model diagram of bilayer COF-O nanosheets with several different offsets of 0%-50%.

Section S10. Two-dimensional density distribution of water molecules in COF-O membrane with different horizontal offsets.

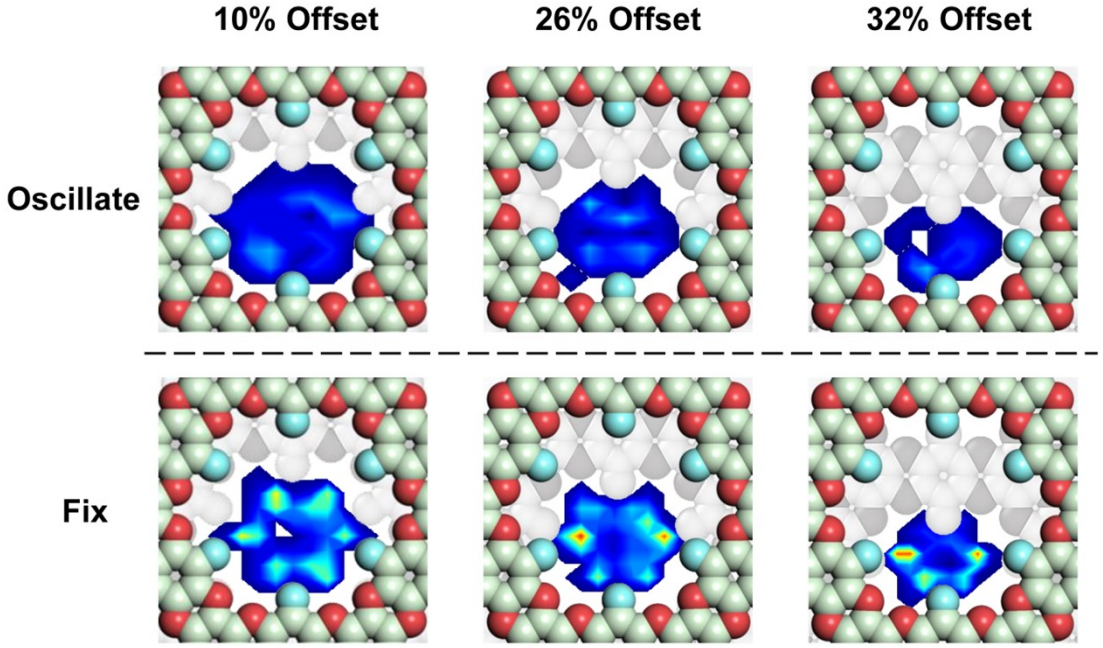

Fig. S16 Water molecules density distribution in the xy plane for fixed membrane (down, A=0 Å, T=0 ps) and oscillated membrane (up, A=1 Å, T=1.0 ps) with 10-32% offsets.

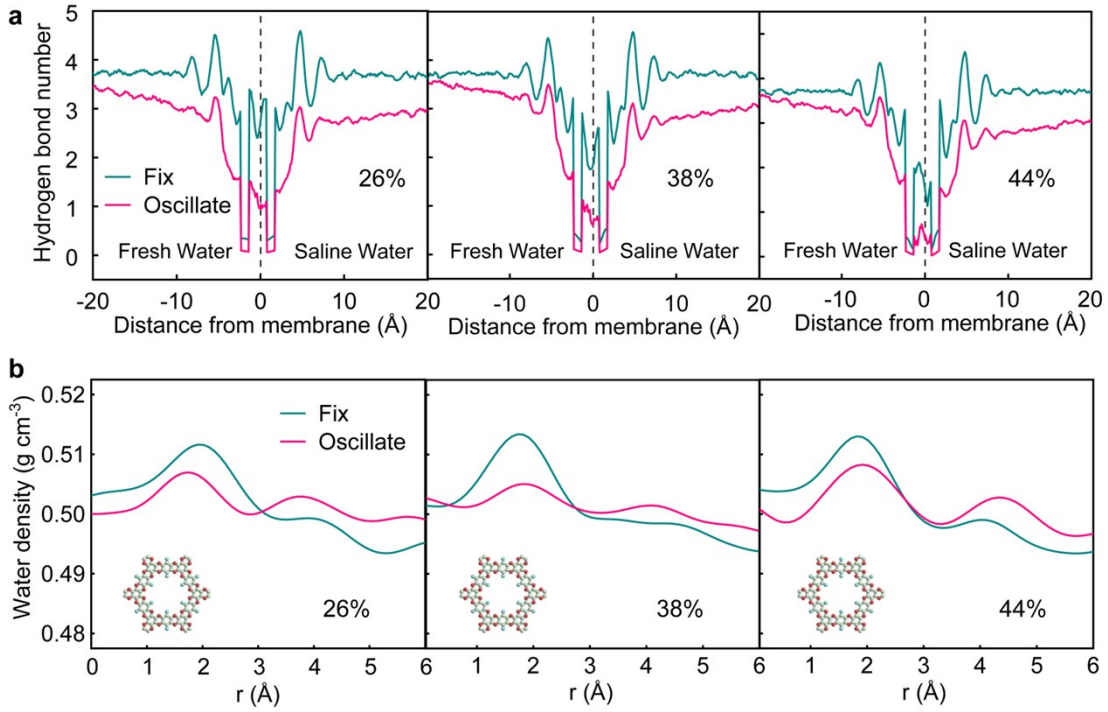

Fig. S17 (a) Average hydrogen bonding distribution along the z-axis for COF-O oscillated membrane (A=1 Å, T=1.0 ps) and the fixed membrane (A=0 Å, T=0 ps) with the offset 26%-44%. (b) Water flux versus pore center distance for COF-O oscillated (A=1 Å, T=1.0 ps) and fixed (A=0 Å, T=0 ps) membranes with the offset 26%-44%.

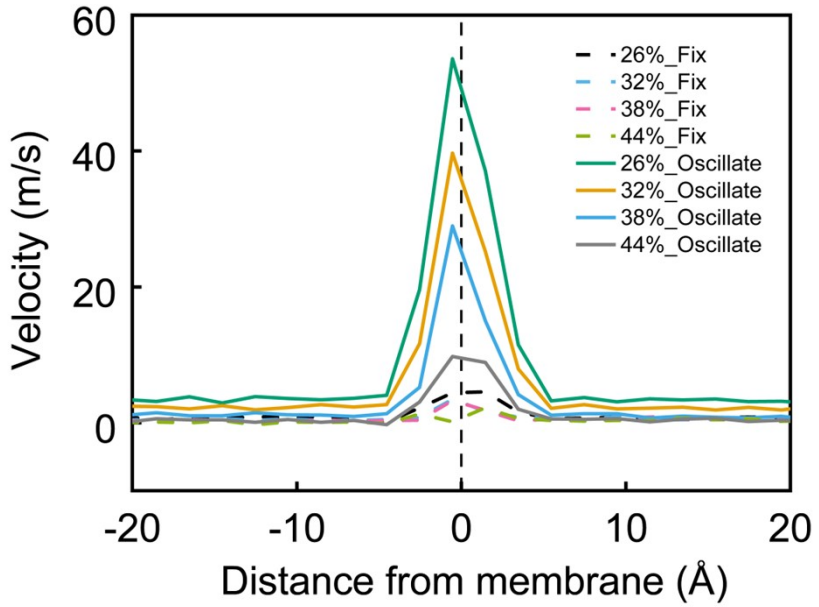

Fig. S18 Water molecules velocity as a function of the distance for different offsets COF-O filtration system.

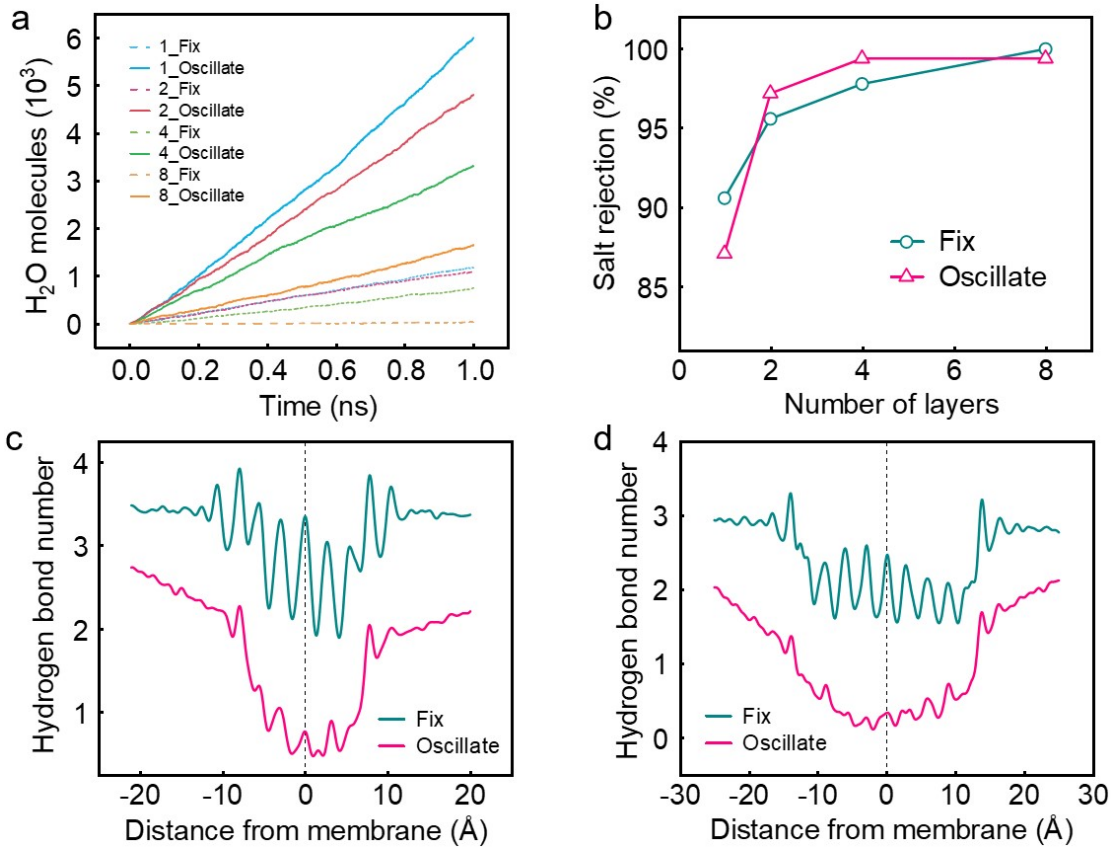

Fig. S19 (a) The amounts of penetrated water molecules as a function of time with different COF-O membranes thicknesses in the oscillated (A = 1 Å, T = 1.0 ps) and fixed (A = 0 Å, T = 0 ps) states. (b) Salt rejection as a function of COF-O membranes thicknesses in the oscillated (A = 1 Å, T = 1.0 ps) and fixed (A = 0 Å, T = 0 ps) states. Average hydrogen bonding distribution along the z-axis for the oscillated and the fixed states for membranes with 4-layer thickness (c) and 8-layer thickness (d).

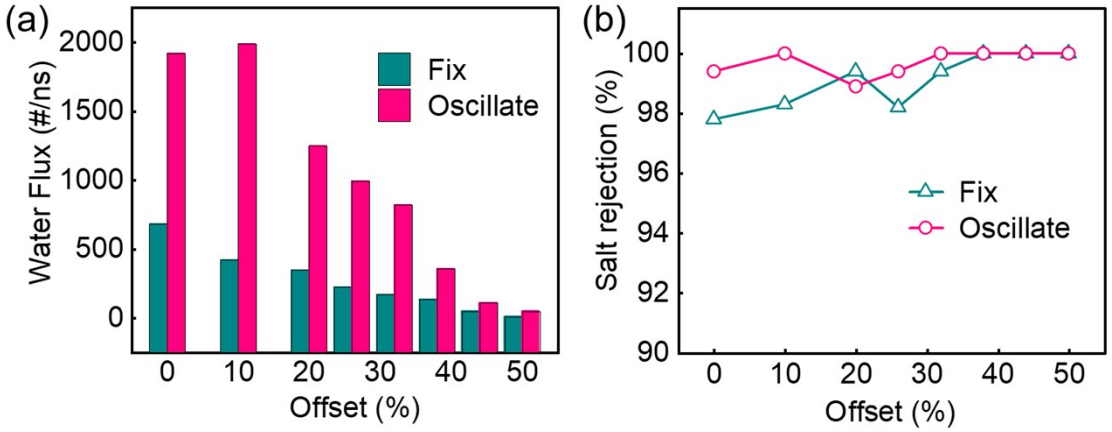

Fig. S20 Variation of water flux (a) and salt rejection rate (b) of bilayer COF-O membranes with different offsets at 50 MPa in oscillated and fixed states.

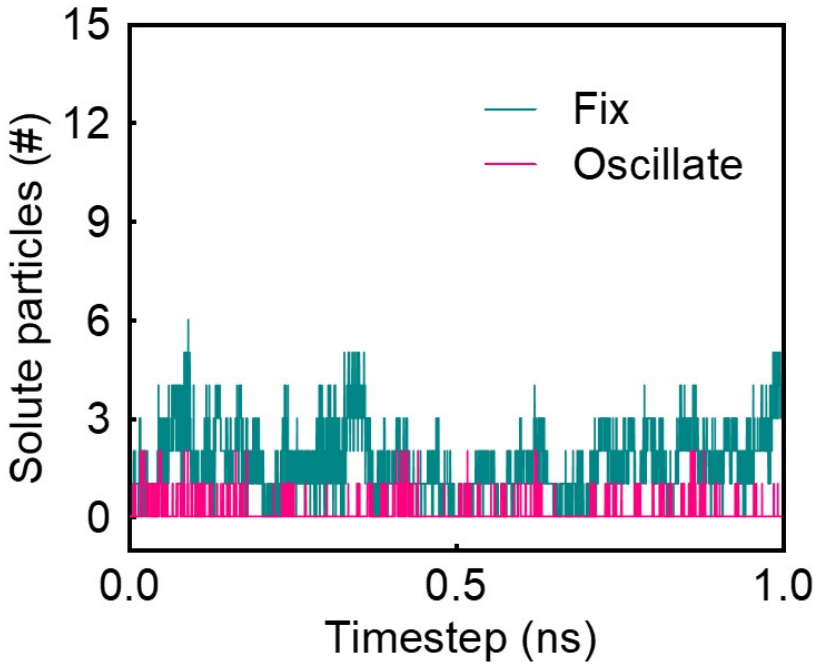

Fig. S21 The number of solute ions adsorbed in the membrane pores as a function of time.

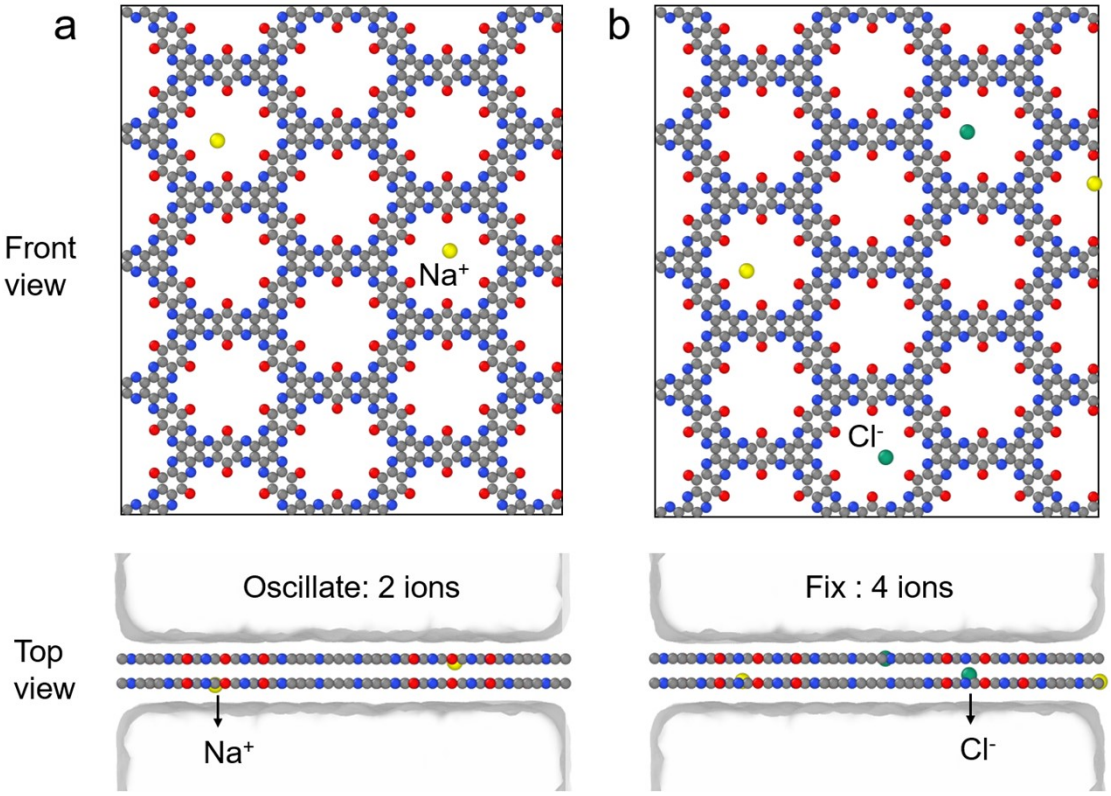

Fig. S22 Simulated snapshots for the oscillated membrane (a) and the fixed membrane (b) with 0% offset COF-O.

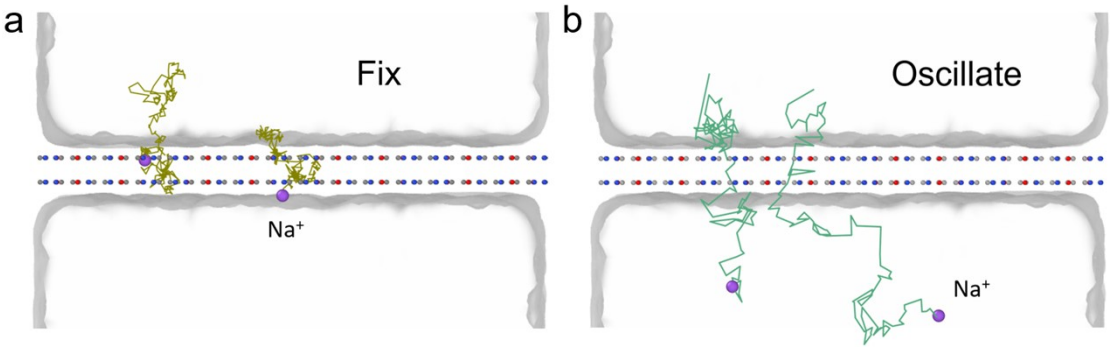

Fig. S23 (a) The trajectories of 2 randomly selected Na^+ passing through the fixed COF-O membrane within 0.2 ns. (b) The trajectories of 2 randomly selected Na^+ passing through the oscillated COF-O membrane within 0.02 ns.

Supporting Table 2. All data in this work are displayed in lists for different amplitudes (0-2.0 Å), periods (0-4.0 ps) and offsets (0-50 %).

Offset (%)	Amplitude: A (Å) Period: T (ps)	Pore Size (nm)	Water flux (L/cm²/day/MPa)	Rejection rate [%]
0%	A=0, T=0	1.20	82.04	96.1
	A=0.5, T=1.0	1.20	220.5	93.3
	A=1.0, T=1.0	1.20	327.88	97.2
	A=1.5, T=1.0	1.20	287.00	98.9
	A=2.0, T=1.0	1.20	355.04	99.4
	A=1.0, T=2.0	1.20	186.34	96.7
	A=1.0, T=3.0	1.20	153.30	96.7
	A=1.0, T=4.0	1.20	106.96	96.7
10%	A=0, T=0	1.12.	59.36	97.8
	A=0.5, T=1.0	1.12.	196.00	96.7
	A=1.0, T=1.0	1.12.	269.36	98.9
	A=1.5, T=1.0	1.12.	274.40	99.4
	A=2.0, T=1.0	1.12.	260.68	99.4
	A=1.0, T=2.0	1.12.	186.48	94.4
	A=1.0, T=3.0	1.12.	145.18	93.1
	A=1.0, T=4.0	1.12.	106.12	97.2
20%	A=0, T=0	1.05	41.06	93.3
	A=0.5, T=1.0	1.05	136.92	96.7
	A=1.0, T=1.0	1.05	205.59	98.3
	A=1.5, T=1.0	1.05	192.15	99.4
	A=2.0, T=1.0	1.05	195.51	99.4
	A=1.0, T=2.0	1.05	139.93	93.9
	A=1.0, T=3.0	1.05	97.72	97.8
	A=1.0, T=4.0	1.05	81.55	94.4
26%	A=0, T=0	0.95	32.49	96.1
	A=0.5, T=1.0	0.95	108.71	98.3
	A=1.0, T=1.0	0.95	165.06	98.9
	A=1.5, T=1.0	0.95	168.14	99.4
	A=2.0, T=1.0	0.95	173.67	100.0
	A=1.0, T=2.0	0.95	139.93	93.9
	A=1.0, T=3.0	0.95	97.72	97.8
	A=1.0, T=4.0	0.95	81.55	94.4
32%	A=0, T=0	0.85	22.792	98.9
	A=0.5, T=1.0	0.85	81.41	98.3
	A=1.0, T=1.0	0.85	113.26	98.9
	A=1.5, T=1.0	0.85	106.82	99.4
	A=2.0, T=1.0	0.85	122.5	100
	A=1.0, T=2.0	0.85	86.59	99.4
	A=1.0, T=3.0	0.85	58.31	99.4

	A=1.0, T=4.0	0.85	50.26	97.8
38%	A=0, T=0	0.75	14.35	98.9
	A=0.5, T=1.0	0.75	49.56	98.9
	A=1.0, T=1.0	0.75	55.09	99.4
	A=1.5, T=1.0	0.75	61.88	100
	A=2.0, T=1.0	0.75	65.31	100
	A=1.0, T=2.0	0.75	52.22	98.3
	A=1.0, T=3.0	0.75	33.46	99.4
	A=1.0, T=4.0	0.75	33.32	98.9
44%	A=0, T=0	0.65	8.022	99.4
	A=0.5, T=1.0	0.65	17.57	100
	A=1.0, T=1.0	0.65	17.50	100
	A=1.5, T=1.0	0.65	24.01	100
	A=2.0, T=1.0	0.65	27.37	100
	A=1.0, T=2.0	0.65	18.97	100
	A=1.0, T=3.0	0.65	15.40	100
	A=1.0, T=4.0	0.65	11.83	99.4